NUCLEIC ACID THERAPEUTICS
Volume 30, Number 2, 2020
Mary Ann Liebert, Inc.
DOI: 10.1089/nat.2019.0811

Systemic Evaluation of Chimeric LNA/2′-O-Methyl Steric Blockers for Myotonic Dystrophy Type 1 Therapy

Melina Christou,[1,2] Jesper Wengel,[3] Kleitos Sokratous,[4,5,*] Kyriacos Kyriacou,[2,4] Georgios Nikolaou,[6] Leonidas A. Phylactou,[1,2] and Nikolaos P. Mastroyiannopoulos[1,2]

Myotonic dystrophy type 1 (DM1) is a dominantly inherited, multisystemic disorder characterized clinically by delayed muscle relaxation and weakness. The disease is caused by a CTG repeat expansion in the 3′ untranslated region (3′ UTR) of the *DMPK* gene, which leads to the expression of a toxic gain-of-function mRNA. The expanded CUG repeat mRNA sequesters the MBNL1 splicing regulator in nuclear-retained foci structures, resulting in loss of protein function and disruption of alternative splicing homeostasis. In this study, we used CAG repeat antisense oligonucleotides (ASOs), composed of locked nucleic acid (LNA)- and 2′-*O*-methyl (2′*O*Me)-modified bases in a chimeric design, to alleviate $CUG^{expanded}$-mediated toxicity. Chimeric 14–18mer LNA/2′*O*Me oligonucleotides, exhibiting an LNA incorporation of ∼33%, significantly ameliorated the misregulated alternative splicing of Mbnl1-dependent exons in primary DM1 mouse myoblasts and tibialis anterior muscles of DM1 mice. Subcutaneous delivery of 14mer and 18mer LNA/2′*O*Me chimeras in DM1 mice resulted in high levels of accumulation in all tested skeletal muscles, as well as in the diaphragm and heart tissue. Despite the efficient delivery, chimeric LNA/2′*O*Me oligonucleotides were not able, even at a high-dosage regimen (400 mg/kg/week), to correct the misregulated splicing of *Serca1* exon 22 in skeletal muscles. Nevertheless, oligonucleotide doses were well-tolerated as determined by histological and plasma biochemistry analyses. Our results provide proof of concept that inhibition of MBNL1 sequestration by systemic delivery of a steric-blocking ASO is extremely challenging, considering the large number of target sites that need to be occupied per RNA molecule. Although not suitable for DM1 therapy, chimeric LNA/2′*O*Me oligonucleotides could prove to be highly beneficial for other diseases, such as Duchenne muscular dystrophy, that require inhibition of a single target site per RNA molecule.

Keywords: DM1, antisense oligonucleotide, LNA, 2′-*O*-methyl, *in vivo*

Introduction

Myotonic dystrophy type I (DM1) is a dominantly inherited, multisystemic disorder characterized clinically by muscle stiffness—a result of delayed muscle relaxation—and progressive weakness [1,2]. Pathology arises from a CTG repeat expansion in the 3′ untranslated region (3′ UTR) of the *dystrophia myotonica protein kinase* (*DMPK*) gene, which transcribes into a toxic gain-of-function mRNA [3]. The unusually long CUG^{exp} region in the mutant transcript folds into a stable hairpin structure and sequesters the splicing regulator muscleblind-like-1 (MBNL1), forming large ribonucleoprotein (CUG^{exp}-MBNL1) aggregates (or foci) inside the nucleus [4]. MBNL1 sequestration leads to its functional depletion in the nucleus and cytoplasm causing missplicing of its own pre-mRNA and other regulatory targets

[1]Department of Molecular Genetics, Function & Therapy, The Cyprus Institute of Neurology and Genetics, Nicosia, Cyprus.
[2]The Cyprus School of Molecular Medicine, The Cyprus Institute of Neurology and Genetics, Nicosia, Cyprus.
[3]Department of Physics, Chemistry and Pharmacy, Biomolecular Nanoscale Engineering Center, University of Southern Denmark, Odense M, Denmark.
[4]Department of Electron Microscopy and Molecular Pathology, The Cyprus Institute of Neurology and Genetics, Nicosia, Cyprus.
[5]Bioinformatics Group, The Cyprus Institute of Neurology and Genetics, Nicosia, Cyprus.
[6]Veterinary Diagnostic Laboratory, Vet Ex Machina Ltd, Nicosia, Cyprus.
*Current affiliation: OMass Therapeutics, Oxford, United Kingdom.

[5–9]. Abnormally expressed embryonic or nonfunctional splice isoforms help explain several multisystemic symptoms of the disease, including cardiac conduction abnormalities—a result of *SCN5A* (*cardiac sodium channel*) and *TNNT2* (*cardiac troponin T type 2*) missplicing [8,10]—and insulin insensitivity—due to aberrant alternative splicing of *IR* (*insulin receptor*) [9].

In the last decade, therapeutic approaches for DM1 have mainly been focused on the use of chemically modified antisense oligonucleotides (ASOs) that either target the expanded repeat tract or bind the mutant *DMPK* mRNA outside the CUG^{exp} region. Depending on the type of chemistry introduced and the design of the antisense construct, ASOs can mitigate RNA toxicity by two possible mechanisms: (1) competing with MBNL1 for CUG^{exp} binding and/or displacing prebound MBNL1 proteins (steric block mechanism); (2) inducing degradation of *DMPK* mRNA via the RNase H machinery. Both mechanisms would result in functional restoration of MBNL1 activity, and consequently, correction of missplicing.

The biggest challenge in ASO development is optimizing the right combination and precise pattern of chemical modifications to be incorporated. Chemical modifications include alterations to the phosphodiester (PO) backbone (eg, phosphorothioate, morpholino), the sugar ring [eg, 2′-*O*-methyl (2′*O*Me), 2′-*O*-methoxyethyl (MOE), locked nucleic acid (LNA), and 2′,4′-constrained ethyl (cEt)], and/or the nucleobases. First-generation ASOs have commonly incorporated the phosphorothioate (PS) modification, which substitutes sulfur for a nonbridging oxygen in the phosphate backbone and confers significant resistance to nuclease degradation [11]. PS linkages are cost-effective, RNase H-compatible modifications that markedly increase ASO binding to plasma proteins, thus improving drug pharmacokinetics [12,13]. Despite increasing ASO stability, PS linkages reduce the binding affinity of an oligonucleotide toward its target sequence, resulting in decreased ASO specificity and potency [11,14]. Importantly, PS-ASOs have also been shown to associate with key cellular proteins (including C23/nucleolin and paraspeckle proteins) in a sequence-independent manner [15–19], a finding that would explain the previously reported side effects of PS oligonucleotides on cells and tissues [20–24]. Indeed, a recent publication by Shen *et al.* provided the first direct evidence that nonspecific binding of known toxic PS-ASOs to paraspeckle proteins results in nucleolar stress, p53 activation, and apoptotic cell death [25].

To counteract the reduced specificity observed with the PS modification, second-generation ASOs have incorporated naturally occurring 2′*O*Me or MOE residues that increase binding affinity for an RNA target and show inherent resistance to cellular endonucleases [13]. 2′-*O*-alkyl-modified ASOs are still susceptible to exonuclease attack and are therefore best used in combination with a small number of PS linkages, at the 3′ and 5′ end, to block both exonuclease and endonuclease degradation. When incorporated in a gapmer design—chemically modified ASO ends flanking a central unmodified region—the 2′-*O*-alkyl modification is compatible with RNase H activity [26]. Nevertheless, *DMPK* mRNA degradation has been reported using a full 2′*O*Me-PS ASO, possibly via an RNase H-independent mechanism [27].

The LNA is a third-generation bicyclic sugar modification, which exhibits unprecedented thermal stability compared with other 2′-chemistries [28,29]. This feature significantly increases the binding affinity of LNA-modified ASOs, but at the same time renders them more tolerant to mismatches, leading to possible off-target interactions [30]. LNA nucleotides are resistant to nuclease degradation and can induce RNase H activity when incorporated in a gapmer design [31]. Owing to their unusually strong binding affinity, LNA monomers have been incorporated in a short (8–12 bp long), all-LNA antisense construct against CUG^{exp} RNA with encouraging results [32]. The 10mer all-LNA ASO reduced the number of RNA^{exp}-MBNL1 foci and specifically corrected MBNL1-sensitive splicing defects in proliferating human DM1 cells and tibialis anterior (TA) muscle of DM1 mice after a single intramuscular injection [32]. Despite encouraging data at the intramuscular level, the short all-LNA ASO has not been evaluated following systemic administration in mice. Importantly, several non-DM1-related studies carrying out short-term tolerability assays in mice have shown that LNA-modified gapmer ASOs are profoundly hepatotoxic [33–35].

The first promising ASO for DM1 therapy, targeting CUG^{exp} RNA outside the repeat tract, was based on an MOE gapmer design with a full PS backbone [36]. Systemic delivery of this second-generation ASO in DM1 transgenic mice resulted in a significant reduction of CUG^{exp} RNA in skeletal muscles, correction of missplicing, and elimination of myotonic discharges, an effect that was sustained for up to 1 year after the last dose [36]. Despite promising preclinical data, the MOE gapmer did not translate into human trials. Ionis Pharmaceuticals and collaborators then proceeded with the development of another RNase H-dependent ASO, modified with the cEt chemistry in a gapmer design. Similar to LNA, cEt residues show significantly increased RNA binding affinity compared with second-generation 2′-*O*-alkyl-modified units. Systemic administration of the cEt gapmer in human *DMPK* transgenic mice or cynomolgus monkeys resulted in up to 70% reduction of *DMPK* mRNA in skeletal muscles and $\sim$50% in cardiac muscle, an effect that was sustained for several months after the end of treatment [37]. This was the first ASO to progress to a phase 1–2 clinical trial for the treatment of DM1; a study that was recently concluded. Although results showed encouraging trends in biomarker and alternative splicing changes, ASO accumulation in muscle tissues did not reach sufficient concentration levels to elicit a significant therapeutic response [38].

RNase H-dependent gapmer ASOs have been well studied in DM1 and have shown great promise for therapy. By contrast, the therapeutic potential of steric-blocking ASOs has been much less explored. Intravenous delivery of a first-generation (morpholino), steric-blocking ASO against CUG^{exp} RNA failed to correct missplicing in skeletal muscles of DM1 transgenic mice [39], while third-generation, all-LNA ASOs did not advance beyond intramuscular evaluation [32]. In this study, we designed and tested the activity of CAG repeat steric-blocking ASOs, of variable sizes, that combine two commonly used high binding affinity modifications in a single antisense construct: the third-generation LNA chemistry, which exhibits unprecedented duplex stability, and the naturally occurring, second-generation 2′*O*Me chemistry, which shows high RNA

binding affinity and inherent resistance to endonuclease degradation. Chimeric LNA/2′*O*Me oligonucleotides have previously been evaluated in microRNA inhibition studies, demonstrating superior potency compared with their LNA- or 2′*O*Me-modified counterparts. The combination of 2′*O*Me monomers with a limited number of LNA nucleotides (one at every third position) aims at minimizing potential toxicity, while retaining a high binding affinity. Furthermore, replacement of the PO backbone with a PS-modified backbone aims at enhancing ASO binding to plasma and cell surface proteins, thus increasing stability and cellular uptake *in vivo* [15,19].

Materials and Methods

Antisense oligonucleotides

All ASOs used in the study are listed in Table 1. Small-scale ASOs used in the *in vitro* experiments were synthesized in the laboratory of Professor Jesper Wengel, while ASOs delivered *in vivo* were purchased from RiboTask ApS. All ASOs bind directly to the expanded CUG repeats but vary in terms of their length (11–18 nucleotides long), the chemistries that they incorporate, and/or the percentage of LNA nucleotides that they hold. Three types of chemical modifications were used: LNA, 2′*O*Me, and PS. The LNA modification was introduced either at the cytosine or the adenine base, specified in the naming as ''LNAc'' or ''LNAa,'' respectively. All ASOs were synthesized on a fully modified PS backbone. In addition to our chimeric LNA/2′*O*Me ASOs, we have included two LNA/DNA mixmer ASOs, ''LNAc/DNA18'' and the previously published ''LNA/DNA18,'' to serve as functional controls.

Animal experiments

All animal studies were carried out at the Transgenic Mouse Facility of the Cyprus Institute of Neurology and Genetics, following evaluation by the ''National Committee for the Protection of Animals Used for Scientific Purposes'' and approval by the Cyprus Veterinary Services (project license approval number: CY/EXP/PR.L2/2014). Homozygous HSA^{LR}20b breeders were kindly provided by Professor Charles A. Thornton of the University of Rochester, United States, while FVB/N mice were purchased from Jackson Laboratories. Intramuscular delivery of ASOs was carried out under tribromoethanol anesthesia (Avertin). Briefly, 4 nmols of ASO was injected into the TA muscle of 2–3-month-old HSA^{LR} mice, followed by electroporation of the treated muscle using previously established parameters (100 V/cm, 20 ms pulse width, 1 Hz, 10 pulses). The contralateral TA was injected with saline only. For systemic delivery, 200 mg/kg of ASO was injected subcutaneously into the interscapular region of 2-month-old female HSA^{LR} mice, twice a week for 4 weeks. ASO pharmacokinetics was studied upon a single subcutaneous injection of the same dose (200 mg/kg). Blood sample collection was carried out from the venous orbital sinus under general anesthesia. Analyses of plasma creatine phosphokinase (CPK), aspartate aminotransferase (AST), alanine aminotransferase (ALT), blood urea nitrogen (BUN), and creatine were carried out by a private Analytical Bioscience Laboratory in Nicosia, Cyprus. All animals were sacrificed by cervical dislocation.

Isolation of single muscle fibers and associated satellite cells

The protocol for isolating satellite cells from single muscle fibers was adapted from Rosenblatt and colleagues [40]. In brief, extensor digitorum longus (EDL) muscles were isolated from 6-week-old HSA^{LR} mice and incubated in 0.2% type I collagenase in Dulbecco's modified Eagle's medium (DMEM, high glucose, pyruvate, no glutamine; Thermo Fisher Scientific), supplemented with 1×penicillin/streptomycin (P-S; Thermo Fisher Scientific) and 1×GlutaMAX solution (Thermo Fisher Scientific), at 37°C for 1 h. Following digestion, single muscle fibers were liberated by repeatedly triturating the EDL muscle using a wide-mouth glass pipette. Viable single muscle fibers were carefully transferred to a new culture dish, in three rounds of washing, to discard hypercontracted fibers and tissue debris. Finally, viable muscle fibers were transferred to a new culture dish coated with 1 mg/mL Matrigel (Corning) in DMEM (1×P-S/1×GlutaMAX) and incubated in ''plating medium'' [DMEM supplemented with 1×P-S, 1×GlutaMAX, 10%

Table 1. Oligonucleotide Nomenclature, Sequence, and Chemistry

ASO name	*Sequence (5′–3′) and modifications*	*LNA %*
LNAc/2′*O*Me18h	**C*** mA* mG* **C*** mA* mG* **C*** mA* mG* **C*** mA* mG* **C*** mA* mG* **C*** mA* mG	33.3
LNAa/2′*O*Me18h	mC* **A*** mG* mC* **A*** mG* mC* **A*** mG* mC* **A*** mG* mC* **A*** mG* mC* **A*** mG	33.3
LNAc/2′*O*Me18ℓ	mC* mA* mG* **C*** mA* mG* mC* mA* mG* **C*** mA* mG* mC* mA* mG* **C*** mA* mG	16.7
LNAc/DNA18	**C*** dA* dG* **C*** dA* dG* **C*** dA* dG* **C*** dA* dG* **C*** dA* dG* **C*** dA* dG	33.3
LNA/DNA18	**C*** dA* **G*** dC* dA* **G*** dC* dA* **G*** dC* dA* **G*** dC* dA* **G*** dC* **A*** **G**	44.4
LNAc/2′*O*Me16	**C*** mA* mG* **C*** mA* mG* **C*** mA* mG* **C*** mA* mG* **C*** mA* mG* **C**	37.5
LNAc/2′*O*Me14	**C*** mA* mG* **C*** mA* mG* **C*** mA* mG* **C*** mA* mG* **C*** mA	35.7
LNAc/2′*O*Me11	**C*** mA* mG* **C*** mA* mG* **C*** mA* mG* **C*** mA	36.3
LNAa/2′*O*Me11	mC* **A*** mG* mC* **A*** mG* mC* **A*** mG* mC* **A**	36.3
LNA/2′*O*Me11	**C*** **A*** mG* mC* mA* mG* mC* mA* mG* **C*** **A**	36.3

The name of each ASO depicts the sugar chemistries that it incorporates (ie, LNA, 2′*O*Me, and/or DNA), the position of the LNA residues (ie, ''LNAc'' = at every cytosine base; ''LNAa'' = at every adenine base), and the number of bases it consists of (11, 14, 16, or 18). Where necessary, the letters ''h'' and ''ℓ'' were added at the end of the name to differentiate same-length ASO counterparts with a high or low LNA percentage, respectively. All ASOs used in the study have a full PS backbone.

Bold and *underlined* = LNA, m = 2′*O*Me, * = PS linkages, d = DNA.

ASOs, antisense oligonucleotides; LNA, locked nucleic acid; 2′OMe, 2′-O-methyl.

horse serum (HS; Thermo Fisher Scientific), and 0.5% chick embryo extract (CEE; MP Biomedicals)] at 37°C for 3 days, to allow myogenic satellite cells to dissociate from their fibers. Three days after plating, the muscle fibers were removed from the dish, and the ''plating medium'' was replaced with ''proliferation medium'' consisting of 20% fetal bovine serum (FBS; Thermo Fisher Scientific), 10% HS, 1% CEE, and 2.5 ng/mL recombinant murine fibroblast growth factor-basic (FGF-b; PeproTech) in DMEM (1 × P-S/1 × GlutaMAX). Myogenic cells were allowed to grow in 5% CO_2 and 37°C for 2–3 days, before plating for transfection.

Cell culture and ASO delivery

Primary HSA^{LR} myoblasts were seeded in 12-well plates coated with 1 mg/mL Matrigel and transfected at 60% confluency in DMEM supplemented with 10% FBS, 1 × P-S, and 1 × GlutaMAX. ASOs were diluted in Opti-MEM™ Reduced Serum Medium (Thermo Fisher Scientific), complexed with Lipofectamine 3000 reagent (Invitrogen), and delivered at a final concentration of 50 nM per well. Cells were collected 24 h post-transfection and processed for RNA extraction using the RNeasy Mini Kit (Qiagen).

DM1 (cell line 10009) human myoblasts were purchased from EuroBioBank and grown in DMEM (high glucose, pyruvate, no glutamine; Thermo Fisher Scientific) supplemented with 20% FBS, 1 × P-S solution (Thermo Fisher Scientific), 1 × GlutaMAX solution (Thermo Fisher Scientific), 10 μg/mL insulin, human recombinant, zinc solution (Thermo Fisher Scientific), 25 ng/mL recombinant human FGF-b (Thermo Fisher Scientific), and 10 ng/mL recombinant human epidermal growth factor (Thermo Fisher Scientific). Cells were incubated in 5% CO_2 at 37°C. For ASO delivery, DM1 myoblasts were seeded in six-well plates so that they would be 60% confluent at the time of transfection. ASOs were diluted in Opti-MEM Reduced Serum Medium, complexed with Lipofectamine 3000 reagent, and delivered at a final concentration of 125 nM per well. Treated cells were either collected for RNA extraction using the RNeasy Mini Kit or seeded on Poly-Prep slides (Sigma) for subsequent fluorescence *in situ* hybridization (FISH), 48 h post-transfection.

Fluorescence in situ *hybridization*

RNA FISH was carried out using a $(CAG)_{10}$ probe labeled with Atto 550 at the 3′-end (Eurofins MWG Operon). Transfected DM1 myoblasts were seeded on Poly-Prep slides (Sigma), fixed in 4% (w/v) paraformaldehyde in phosphate-buffered saline (PBS) for 15 min at 4°C, washed three times in PBS for 5 min at room temperature, permeabilized in 0.4% Triton X-100 for 5 min at room temperature, and washed three times in PBS for 5 min at room temperature. Cells were prehybridized in 40% deionized formamide/2 × SSC in PBS for 15 min at room temperature followed by hybridization in buffer containing 1 ng/μL probe, 40% deionized formamide, 10% dextran sulfate, 1 mg/mL salmon sperm DNA, 1 mg/mL yeast tRNA, 0.2% BSA, 2 mM vanadyl ribonucleoside complex, and 2 × SSC, for 2 h at 50°C. Posthybridization, washes were carried out in 40% deionized formamide/2 × SSC in PBS for 30 min at 53°C, followed by 2 × SSC in PBS for 30 min at 43°C. Cells were counterstained with DAPI II mounting medium and visualized on a Zeiss fluorescent microscope equipped with the AxioCam MRm Zeiss camera. The number of nuclear-retained foci was counted in at least 180 nuclei from two independent transfection experiments.

To carry out FISH on muscle tissue sections, quadriceps muscles were snap-frozen in liquid nitrogen-cooled isopentane and stored at −80°C. Frozen tissues were cryosectioned in the coronal plane, at 5-μm thickness, and collected at 100-μm intervals. Tissue cryosections were fixed in cold 4% paraformaldehyde in PBS for 10 min at room temperature, washed three times in PBS for 5 min, permeabilized in prechilled 1:1 acetone/methanol mixture for 10 min at −20°C, and washed three times in PBS for 5 min. Tissue sections were prehybridized in 50% deionized formamide/4 × SSC in PBS for 10 min at room temperature followed by hybridization in a buffer containing 1 ng/μL probe, 50% deionized formamide, 4 × SSC, 10% dextran sulfate, 0.1 mg/mL salmon sperm DNA, 1 mg/mL yeast tRNA, 0.1% BSA, and 2 mM vanadyl ribonucleoside complex, for 2 h at 40°C. Tissue sections were then washed twice in 1 × SSC in PBS for 20 min at 55°C, and once in 0.5 × SSC in PBS for 15 min at 55°C. Nuclear counterstaining was carried out in Hoechst solution (1:10,000) for 5 min at room temperature, followed by two washes in PBS for 5 min. Tissue sections were visualized under a TCSL confocal microscope (Leica, Germany).

Semiquantitative alternative splicing assays

Total RNA was extracted from untransfected and ASO-transfected myoblasts (human DM1 and primary HSA^{LR}) using the RNeasy Mini Kit (Qiagen). First-strand cDNA was synthesized using 500–1,000 ng total RNA, 0.25 mM dNTPs, 0.75–3 μM random hexamer primers (MWG-Biotech), 200 U M-MuLV reverse transcriptase (NEB), and 1 × M-MuLV transcription buffer (NEB), at 37°C for 1 h. Alternative splicing of *hMBNL1* and m*Mbnl1* exon 7 was assessed by polymerase chain reaction (PCR) amplification of cDNA, using upstream (5′-GCTGCCCAATACCAGGTCAAC-3′) and downstream (5′-TGGTGGGAGAAATGCTGTATGC-3′) primers that bind to exon 6 and 8, respectively. These primers generate either a 216-bp fragment, lacking exon 7, or a 270-bp fragment, which includes exon 7. After 27–28 cycles of amplification, PCR products were electrophoretically resolved on 1.8% agarose gels and visualized by ethidium bromide staining. Band intensities were measured using ImageJ software and the percentage of exon 7 inclusion was calculated in Microsoft Excel. PCR experiments involved three independent transfection replicates.

To assess alternative splicing changes following *in vivo* ASO delivery, skeletal muscle tissues were isolated and homogenized in TRIzol reagent (Ambion). Total RNA was then extracted according to the manufacturer's instructions, treated with DNAse 1 (NEB) and further purified using acid phenol:chloroform (1:1) extraction. First-strand cDNA was synthesized using 1,000 ng total RNA, 0.5 mM dNTPs, 6 μM random primer mix (NEB), 200 U M-MuLV reverse transcriptase (NEB), and 1 × M-MuLV transcription buffer (NEB), at 42°C for 1 h. Alternative splicing of *mSerca1* exon 22 and m*Mbnl1* exon 7 was assessed by PCR amplification of cDNA using upstream (for *mSerca1*: 5′-GCTCAT GGTCC TCAAGATCTCAC-3′, for *mMbnl1*: see paragraph above) and downstream (for *mSerca1*: 5′-GGGTCAGTGCCTCAGCTT TG-3′, for *mMbnl1*: see paragraph above) primers, for 21 and

24 cycles, respectively. PCR products were electrophoretically resolved on 5% polyacrylamide gels, stained with SYBRSafe (Thermo Fisher Scientific), and analyzed using ImageJ.

Quantification of ASOs in mouse plasma and tissues using liquid chromatography tandem mass spectrometry

Quantification of LNAc/2′*O*Me18h and LNAc/2′*O*Me14 ASOs in the skeletal muscle (TA, quadriceps, and gastrocnemius), diaphragm, heart, liver, and kidney tissues was carried out by liquid chromatography with tandem mass spectrometry (LC-MS/MS), as previously described in Goyenvalle *et al.* In brief, ~50 mg of tissue was isolated and homogenized in 1 mL of proteinase K buffer (100 mM Tris-HCl, pH 8.5, 200 mM NaCl, 5 mM EDTA, and 0.2% SDS) containing 2 mg/mL of proteinase K (Roche Applied Science). To enhance enzyme activity, the samples were incubated at 55°C for 2 (liver) or 4 h (kidney, heart, diaphragm, and skeletal muscle) and then centrifuged at 16,000*g* for 15 min. The supernatant was collected and prepared for LC-MS/MS analysis by solid-phase extraction (SPE) on Oasis HLB cartridges (10 mg; Waters, United Kingdom). First, 100 μL of the supernatant sample was spiked with 100 μL of internal standard (IS) solution (0.025 mg of 16mer LNAc/2′*O*Me16 ASO in 100 mM triethylammonium bicarbonate buffer) and incubated at room temperature for 30 min. The SPE cartridges were preconditioned with 1 mL of methanol followed by 2 × 500 μL of buffer A [100 mM 1,1,1,3,3,3-hexafluoro-2-propanol (HFIP; Honeywell Fluka) and 8.6 mM triethylamine (TEA; Sigma) in ultrapure water]. Subsequently, 200 μL of buffer A was added to the ASO-IS mixture and the sample was loaded on the SPE cartridge. The cartridges were washed twice with 250 μL of buffer A and once with 300 μL of 100 mM triethylammonium bicarbonate. ASO elution was carried out using 2 × 200 μL of 40% buffer A in methanol. The samples were dried in a rotational vacuum concentrator (RVC 2–25 CDplus, CHRIST) coupled to a freeze dryer (Alpha 1–4 LSCbasic, CHRIST) and solubilized in 50 μL mobile phase A (15 mM TEA/400 mM HFIP) just before LC-MS/MS analysis.

Sample analysis was performed on a Xevo TQD MS instrument (Waters), coupled to an Acquity UPLC I-class system (Waters), and operated in the negative ion multiple reaction monitoring (MRM) mode (capillary voltage −2.9 kV, source temperature 400°C). Chromatographic separations were carried out on an Acquity BEH OST C18 1.7 μm, 2.1 × 100 mm analytical column (Waters) with gradient elution using mobile phase A and mobile phase B (50% mobile phase A, 50% methanol). Gradient elution was performed at a flow rate of 200 μL/min, starting with 42% B, followed by a linear increase to 66% within 4 min and then to 80% within the next 1 min. The column temperature was kept at 60°C throughout the analyses.

The concentrations of the experimental ASOs (LNAc/2′*O*Me18h and LNAc/2′*O*Me14) and IS ASO (LNAc/2′*O*Me16) were determined according to the peak area ratios $A_{Analyte}/A_{IS}$ for the following MRM transitions: LNAc/2′*O*Me18h $[M\text{-}9H]^{9-}$, *m/z* 711.5 > 346.1; LNAc/2′*O*Me16 $[M\text{-}9H]^{9-}$, *m/z* 629.9 > 346.0; LNAc/2′*O*Me14 $[M\text{-}8H]^{8-}$ *m/z* 618.5 > 346.2 (additional transitions for each precursor ion were used as confirmation ions, see Supplementary Table S1). Calibration was based on a twofold serial dilution of all three ASOs (LNAc/2′*O*Me18h, LNAc/2′*O*Me14, and LNAc/2′*O*Me16) in mobile phase A, over a concentration range of 3.9–1,000 μg/mL.

Drug pharmacokinetics was studied upon a single subcutaneous injection of 200 mg/kg of the respective ASO, followed by blood collection at 0, 30, 60, 90, and 120 min postinjection. A fixed volume of plasma (15 μL) was isolated from each blood sample and spiked with 0.05 mg of IS ASO (LNAc/2′*O*Me16). Plasma samples were then treated with 200 μL of 5% ammonium hydroxide solution, mixed together by vortexing for 10 min, to denature plasma proteins and displace ASO molecules from their binding sites. An equal volume (200 μL) of cold PCA buffer (phenol:chloroform:isoamyl alcohol, 25:24:1; Sigma) was then added to the sample, mixed by vortexing for 10 min, and then centrifuged at maximum speed for 10 min. The aqueous phase was carefully collected and mixed with an equal volume of 100 mM TEA bicarbonate solution for 30 min, to allow ion-pair formation between the ASOs and triethylammonium ions. The SPE method and LC-MS/MS analysis that followed are the same as described for the biodistribution study.

Histology

ASO toxicity was evaluated in the liver and kidney tissues of HSA^{LR} mice treated with 200 mg/kg of the respective ASO, twice a week for 4 weeks. Liver and kidney tissue samples were isolated 2 days after the last dose, fixed overnight in 4% PFA, and embedded in paraffin. The samples were sectioned, stained with hematoxylin and eosin, and examined blindly by a single veterinary pathologist.

Statistical analysis

Data are expressed as mean ± standard error, unless otherwise specified. Statistical significance was calculated using two-tailed unpaired *t*-test, followed by Bonferroni correction.

Results

Activity of chimeric LNA/2′OMe ASOs in vitro

To determine whether ASO delivery can improve splicing misregulation in primary HSA^{LR} myoblasts, we examined *Mbnl1* alternative splicing changes in transfected and untransfected cells by two-step reverse transcription-PCR (RT-PCR). MBNL1 is a ubiquitously expressed splicing factor that autoregulates the alternative splicing of its own pre-mRNA. In healthy cells, increased nuclear MBNL1 activity enhances exon 7 skipping, resulting in *MBNL1* isoforms that lack the nuclear localization signal (Fig. 1A) [7]. Reduced nuclear MBNL1 activity may in turn enhance exon 7 inclusion leading to MBNL1 nuclear localization. This feedback autoregulation is crucial for maintaining MBNL1 function in the nucleus [7]. In DM1 myoblasts, functional depletion of nuclear MBNL1 leads to enhanced exon 7 inclusion resulting in abnormal nuclear MBNL1 accumulation and enhanced CUG^{exp}-MBNL1 interaction [7]. Correcting MBNL1 alternative missplicing will restore its function in the nucleus leading to correct splicing of other regulatory targets.

Our 18mer, 16mer, and 14mer chimeric LNA/2′*O*Me ASOs (LNAc/2′*O*Me18h, LNAa/2′*O*Me18h, LNAc/2′*O*Me16, and LNAc/2′*O*Me14), exhibiting a relatively high LNA

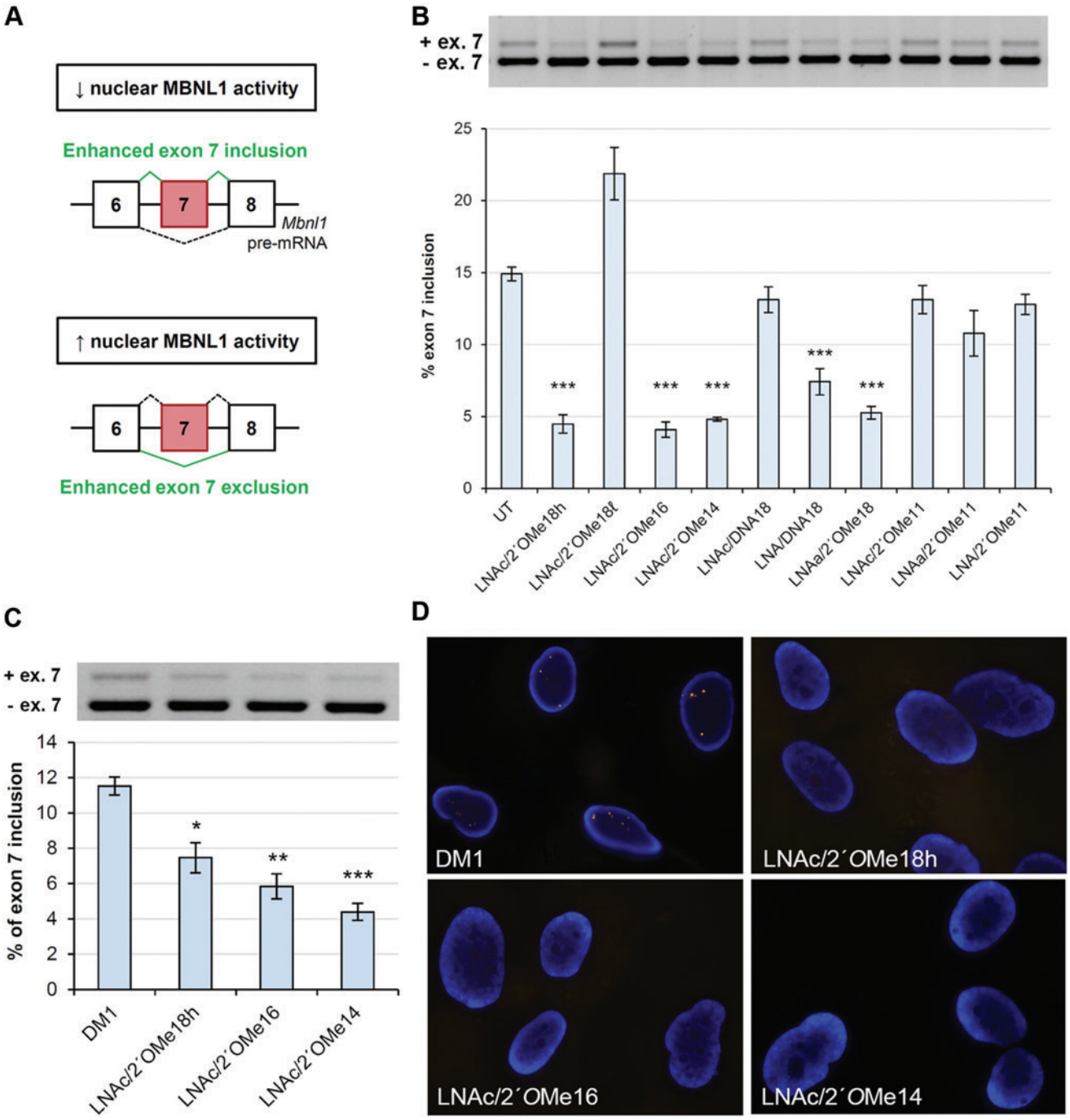

FIG. 1. Chimeric LNA/2′*O*Me ASOs ameliorate *Mbnl1* alternative missplicing *in vitro*. **(A)** Schematic diagram illustrating *MBNL1* alternative splicing autoregulation. Functional depletion of nuclear MBNL1 leads to enhanced exon 7 inclusion, while an increase in nuclear MBNL1 protein activity enhances exon 7 exclusion. **(B)** RT-PCR analysis of *Mbnl1* alternative splicing changes in primary HSA^{LR} myoblasts treated with Lipofectamine reagent only (UT) or 50 nM of the respective ASO. Total RNA was extracted 24 h post-transfection. **(C)** RT-PCR analysis of *MBNL1* alternative splicing changes in human DM1 myoblasts treated with Lipofectamine reagent only (DM1) or 125 nM of the respective ASO. Total RNA was extracted 48 h post-transfection. **(D)** Representative FISH images of untransfected (DM1) and ASO-treated human DM1 myoblasts. Cells were treated with 125 nM ASO and collected for FISH analysis 48 h post-transfection. Blue = DAPI nuclear staining; yellow = CUG^{exp}-MBNL1 foci. Values are mean ± S.E.M. from three transfection experiments. *Denotes $P < 0.05$, **denotes $P < 0.01$, ***denotes $P < 0.001$ compared with UT using the two-sample *t*-test followed by Bonferroni correction. ASO, antisense oligonucleotide; FISH, fluorescence *in situ* hybridization; 2′*O*Me, 2′-*O*-methyl; RT-PCR, reverse transcription polymerase chain reaction. Color images are available online.

incorporation (33%–38%), significantly ameliorated *Mbnl1* exon 7 missplicing in primary HSA^{LR} myoblasts (Fig. 1B). Control LNA/DNA18 mixmer, which contains the largest number of LNA nucleotides among all tested ASOs, was less potent than our 14–18mer LNA/2′*O*Me chimeras, but still significantly reduced the levels of exon 7-included *Mbnl1* transcript in primary HSA^{LR} myoblasts. By contrast, control LNAc/DNA18 mixmer, with an LNA incorporation of 33.3%, and LNAc/2′*O*Me18ℓ, containing half the number of LNA residues than all other tested ASOs, did not improve the misregulated splicing of *Mbnl1* exon 7. These results suggest that (1) the combination of LNA and 2′*O*Me monomers in a single antisense construct greatly enhances ASO potency compared with LNA-containing ASOs; and (2) an LNA incorporation of ∼33%, evenly distributed at every third position, shows the most potent results. Importantly, our 11mer LNA/2′*O*Me chimeras exhibiting a high LNA incorporation (36.3%) did not improve *Mbnl1* missplicing, suggesting that the combination of LNA and 2′*O*Me chemistries in very short ASO designs does not enable sufficient target binding to achieve an effect.

To further evaluate ASO activity, LNAc/2′*O*Me18h, LNAc/2′*O*Me16, and LNAc/2′*O*Me14 chimeras were complexed with the Lipofectamine reagent and delivered in proliferating human DM1 myoblasts. All three ASOs were able to completely eliminate nuclear-retained CUG^{exp}-MBNL1 foci and significantly improve *MBNL1* exon 7 missplicing in human DM1 myoblasts, after 48 h of treatment (Fig. 1C, D). Unexpectedly, we observed that ASO activity increased with reduced ASO size. A possible explanation would be that a larger number of 14mer molecules can be accommodated per nucleic acid/cationic lipid complex than a 16mer or 18mer ASO. This trend was not seen following transfection of ASOs in primary HSA^{LR} myoblasts, probably due to differences in the efficiency of lipofection between the various cell lines.

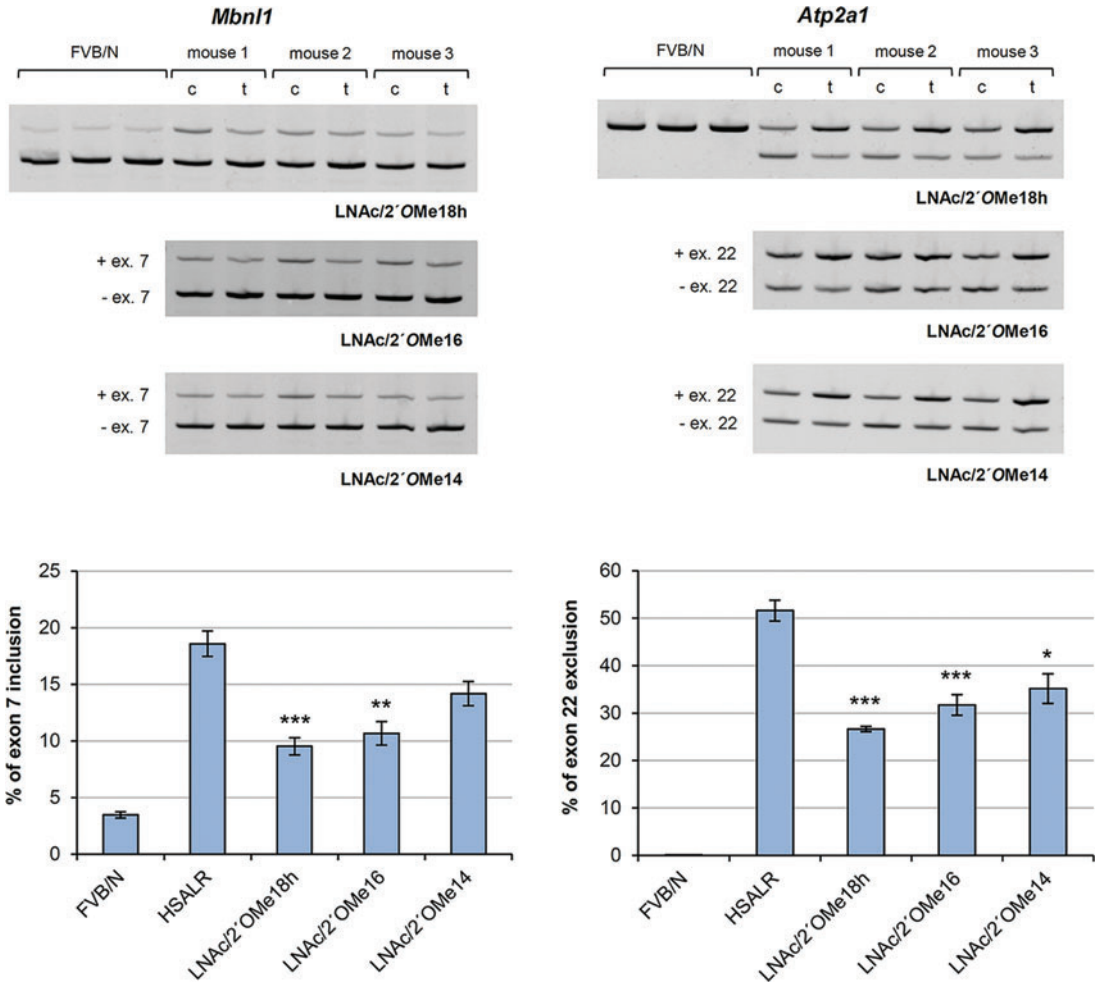

FIG. 2. Partial reversal of misregulated alternative splicing after intramuscular delivery of chimeric LNA/2′*O*Me ASOs. RT-PCR analysis of alternative splicing changes for *Mbnl1* and *Serca1* in TA muscles of 2–3-month-old HSA^{LR} mice, sacrificed 2 weeks after treatment (t) with 4 nmol of one of the three LNA/2′*O*Me chimeras ($n=3$ per tested ASO). The contralateral (c) TA was injected with saline only. Splice products from TA muscles of age-matched wild-type (FVB/N) mice ($n=3$) are also shown. Quantification of results is expressed as the percentage of splice variant that includes or excludes the indicated exon. Values are mean ± S.E.M. *Denotes $P<0.05$, **denotes $P<0.01$, ***denotes $P<0.001$ compared with saline controls using the two-sample *t*-test followed by Bonferroni correction. TA, tibialis anterior. Color images are available online.

Activity of chimeric LNA/2′OMe ASOs after intramuscular delivery

Following *in vitro* screening, we progressed to intramuscular delivery with the three most potent ASOs—LNAc/2′–*O*Me18h, LNAc/2′*O*Me16, and LNAc/2′*O*Me14. All three oligomers have the same percentage of LNA-modified nucleotides but vary in size. The ASOs were delivered locally into the TA muscle of HSA^{LR} mice and electroporated to facilitate cellular uptake. Tissues were isolated 2 weeks post-treatment and alternative splicing regulation was assessed by RT-PCR analysis. The 18mer, 16mer, and 14mer LNA/2′*O*Me chimeras were able to reverse the misregulated alternative splicing of *Mbnl1* exon 7 and *Serca1* exon 22 by ~50%, 40%, and 28%, respectively (Fig. 2). As expected, LNAc/2′*O*Me18h showed the highest potency *in vivo*, a result that contrasts to what we observed in cultured human DM1 myoblasts. A possible explanation would be the difference in the method—chemical versus physical—of ASO delivery. While cationic lipid-mediated transfection (chemical method) in cultured cells may be more sensitive to ASO size, thus favoring shorter nucleic acid molecules (see 'Activity of chimeric LNA/2'OMe ASOs in vitro' in the 'Results' section), ASO delivery by *in vivo* electroporation (physical method) may be less affected by molecular size.

Pharmacokinetics, biodistribution, and activity of chimeric LNA/2′OMe ASOs following subcutaneous delivery

Drug pharmacokinetics was studied upon a single subcutaneous injection of 200 mg/kg of the respective ASO. Plasma levels of LNAc/2′*O*Me18h and LNAc/2′*O*Me14 rose rapidly within the first 30 min post injection, but continued to increase at a slower rate over the next 90 min (Fig. 3A). This is consistent with a relatively slow absorption rate of biomolecules administered via the subcutaneous route. To study biodistribution, 2-month-old HSA^{LR} female mice were treated with 200 mg/kg of one of the two ASOs—LNAc/2′*O*Me18h and LNAc/2′*O*Me14—or saline only, two times a week for 4 weeks. Skeletal muscles (TA, quadriceps, and gastrocnemius), diaphragm, heart, liver, and kidney tissues were isolated 2 days after the last dose and processed for LC-MS/MS analysis for the detection and quantification of the respective ASOs. Chimeric LNA/2′*O*Me ASOs accumulated in all tested skeletal muscles, as well as in the diaphragm and heart tissue (Fig. 3B). As expected, both ASOs accumulated to highest levels in the liver and kidneys, while size difference did not appear to affect ASO clearance. To assess the effect of ASO treatment on Mbnl1-dependent splicing misregulation, all three skeletal muscles were processed for RNA extraction and RT-PCR analysis of *Serca1* splice variants. Unfortunately, even at this high-dosage regimen, our chimeric LNA/2′*O*Me ASOs did not correct the misregulated splicing of *Serca1* exon 22 (Fig. 4A). Consistent with these data, FISH analysis of quadriceps muscle tissue from ASO-treated HSA^{LR} mice revealed no decrease in the number or intensity of nuclear-retained CUG^{exp}-Mbnl1 foci compared with saline-treated controls (Fig. 4B).

Toxicity status of chimeric LNA/2′OMe ASOs in vivo

To determine the safety of chimeric LNA/2′*O*Me ASOs *in vivo*, body and tissue weights, as well as plasma markers of hepatic injury or renal function, were measured after treatment with 200 mg/kg of the indicated ASO, twice a week for 4 weeks. Body weights, as well as the weights of spleen, liver and kidney tissues, were similar between ASO- and saline-treated HSA^{LR} mice (Fig. 5A). Studies of hepatic cytotoxic markers showed slightly elevated levels of AST in LNAc/2′*O*Me18h- and LNAc/2′*O*Me14-treated HSA^{LR} mice compared with saline controls, and similar levels of ALT in all ASO-treated and untreated mice (Fig. 5B). Plasma CPK, a marker of muscle damage, was reduced in all ASO-treated HSA^{LR} mice, particularly with ASO LNAc/2′*O*Me14 administration. Studies of renal function showed similar levels of creatinine in all ASO-treated and untreated mice, and slightly elevated levels of BUN in LNAc/2′*O*Me18h-treated HSA^{LR} mice, compared with saline controls.

ASO safety was further assessed by histological analysis of liver and kidney sections stained with hematoxylin and eosin (Fig. 5C). The majority of sections examined, from both control and ASO-treated HSA^{LR} mice, exhibited mild

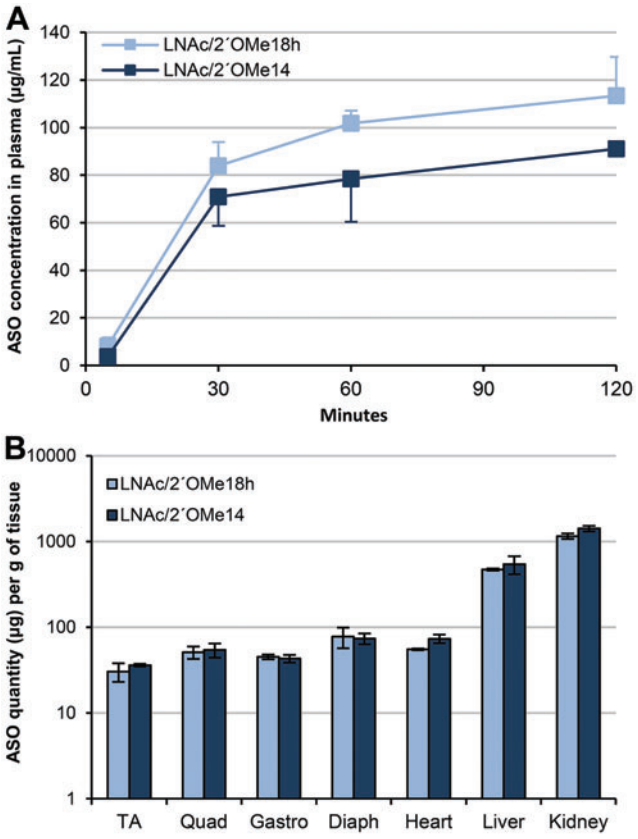

FIG. 3. Pharmacokinetics and biodistribution of chimeric LNA/2′*O*Me ASOs. **(A)** Pharmacokinetics of LNAc/2′*O*Me18h and LNAc/2′*O*Me14 after a single subcutaneous injection of 200 mg/kg. Plasma levels of the two ASOs were determined by LC-MS/MS. **(B)** Tissue levels of LNAc/2′*O*Me18h and LNAc/2′*O*Me14 following a 4-week treatment at 400 mg/kg/week. Skeletal muscles (TA, quadriceps, and gastrocnemius), diaphragm, heart, liver, and kidney tissues were isolated 2 days after the last dose and processed for LC-MS/MS analysis. $n = 3$ per tested ASO. Values are expressed as the mean ± S.E.M. LC-MS/MS, liquid chromatography tandem mass spectrometry. Color images are available online.

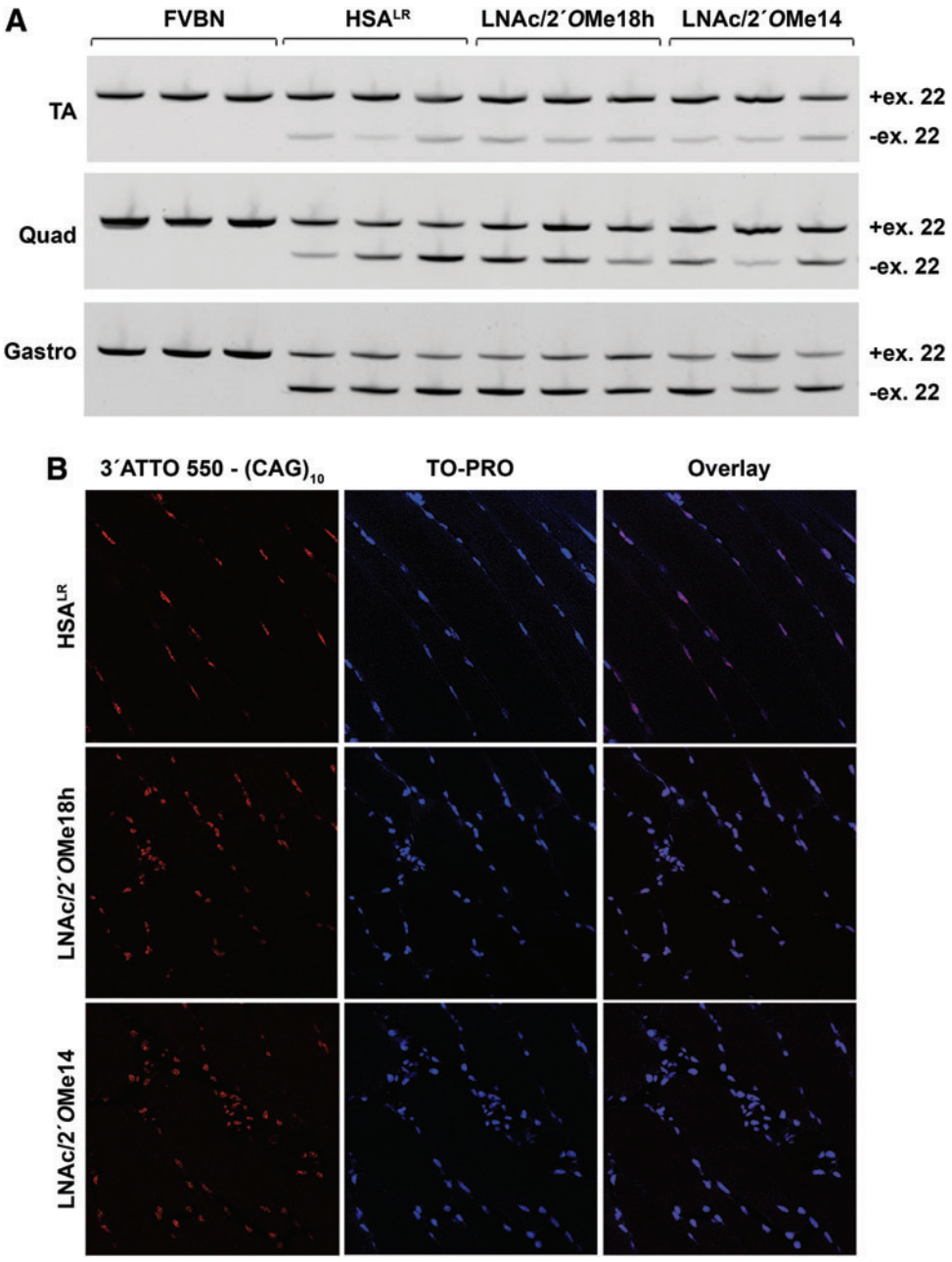

FIG. 4. **(A)** RT-PCR analysis of alternative splicing of *Serca1* transcript in 3-month-old FVB/N wild-type mice ($n=3$) and age-matched HSA^{LR} mice treated with the indicated ASO by subcutaneous injection of 200 mg/kg, biweekly for 4 weeks ($n=3$ per ASO tested). Skeletal muscles (TA; quadriceps, quad.; gastrocnemius, gastro.) were isolated 2 days after the final dose. Age-matched saline-injected HSA^{LR} mice were included as controls ($n=3$). In wild-type mice, there is 100% inclusion of *Serca1* exon 22 in the final transcript, while in HSA^{LR} mice, functional depletion of Mbnl1 results in repression of exon 22 inclusion and expression of the neonatal form of Serca1 (Serca1b) that has reduced Ca^{2+}-dependent ATPase activity. No detectable improvement in *Serca1* exon 22 missplicing was observed after subcutaneous delivery of 200 mg/kg ASO. **(B)** Detection of CUG^{exp}-Mbnl1 foci in frozen quadriceps muscle sections of HSA^{LR} mice treated with the indicated ASO by subcutaneous injection of 200 mg/kg, biweekly for 4 weeks. Tissues were isolated 2 days after the final dose. CUG^{exp} RNA was detected by FISH using a $(CAG)_{10}$ repeat oligonucleotide probe 3′ labeled with ATTO 550. TO-PRO counterstaining was carried out to visualize nuclei. Representative images from each group are shown. Magnification = 40× objective with 1.5× digital zoom. Color images are available online.

hyperemia probably due to the fact that no animal perfusion had been carried out before tissue isolation. Assessment of renal tissue sections revealed no histological abnormalities in saline- and LNAc/2′*O*Me18h-treated HSA^{LR} mice, while in two mice injected with LNAc/2′*O*Me14, we observed acute mild necrosis affecting ~10% of the proximal convoluted tubules. Assessment of liver sections revealed randomly distributed necrosis in ~10% of hepatocytes in two mice injected with LNAc/2′*O*Me18h. A single lesion of perivascular lymphocytic infiltration was also observed in one of the

two mice, an event that could also be random. Importantly, there was one LNAc/2′*O*Me18h-treated mouse that showed no histological abnormality, similar to HSA^{LR} controls. Liver sections of LNAc/2′*O*Me14-injected mice exhibited diffuse, mild-to-moderate vacuolation and mild hepatocellular necrosis.

Discussion

DM1 is a highly complex disease that affects multiple organs and systems in the body. The primary pathologic mechanism is the sequestration of MBNL1 protein by the CUG^{exp} repeat tract, leading to loss of nuclear MBNL1-dependent splicing regulation. Therapeutic research in the last decade has mainly been concentrating on the use of chemically modified ASOs that inhibit protein sequestration to the repeat site and thus restore MBNL1 function in the nucleus. Chemical alterations to the 2′-hydroxyl position of the ribose sugar—2′*O*Me, MOE, LNA, and cEt—have been particularly appealing for antisense applications as they increase target binding affinity, stability, and pharmacokinetics *in vivo*. In this study, we combined two of the most commonly used sugar modifications in a chimeric design to help offset potential negative effects, while retaining a high target binding affinity.

Our chimeric LNA/2′*O*Me ASOs act by directly competing with MBNL1 for CUG binding to restore protein function. At the cellular level, we have proven that the combination of LNA and 2′*O*Me nucleotides in an 18mer ASO construct (LNAc/2′*O*Me18h, LNAa/2′*O*Me18h) is more potent than an LNA/DNA mixmer of the same length and LNA composition (LNAc/DNA18). However, when introduced in short (11mer) antisense constructs, the combination of LNA and 2′*O*Me nucleotides was ineffective in correcting *Mbnl1* exon 7 missplicing in primary HSA^{LR} myoblasts. By contrast, a 10mer ASO, with a fully modified LNA sugar core, has previously been shown to significantly correct MBNL1-sensitive splicing defects in proliferating human DM1 cells and TA muscle of HSA^{LR} mice [32]. Considering that LNA monomers have superior binding affinity compared with 2′*O*Me nucleotides and that reduced ASO lengths compromise hybridization stability, a fully modified LNA sugar core would theoretically be more beneficial than an LNA/2′*O*Me combination when designing short antisense constructs. However, the LNA/2′*O*Me combination can be used to make longer (14mer–18mer), fully modified ASOs with high binding affinities and potentially reduced off-target annealing. The impact of LNA nucleotide inclusion on the efficacy of truncated exon-skipping oligonucleotides has previously been demonstrated in an *in vitro* study by Le *et al.* While an 18mer 2′*O*Me-PS ASO with a two-nucleotide truncation was able to maintain exon 23 skipping efficiency *in vitro*, further reductions in ASO size significantly reduced the efficacy, with 12mer and 14mer variants showing no activity at all [41]. Importantly, the introduction of four LNA nucleotides in the 14mer, 16mer, and 18mer 2′*O*Me-PS ASOs significantly improved the yield of exon 23 skipped RNA product, thus demonstrating that shorter ASOs with high steric-blocking activities can be constructed by combining LNA and 2′*O*Me-PS nucleotides [41].

When delivered locally into the TA muscle of HSA^{LR} mice, LNAc/2′*O*Me18h, LNAc/2′*O*Me16, and LNAc/2′*O*Me14 ASOs were able to partially reverse the misregulated alternative splicing of *Serca1* exon 22 and *Mbnl1* exon 7. As expected, LNAc/2′*O*Me18h was the most potent ASO, since a single 18mer molecule can occupy and block a larger $(CUG)_n$ target region in the mutant mRNA (it is worth rementioning that we injected equimolar doses of the three ASOs into the TA muscle). Although our results clearly demonstrate partial reversal of misregulated spliced exons, the efficacy of our chimeric ASOs appears to be lower than that reported for other steric-blocking ASOs—25mer morpholino and 10mer all-LNA—at the intramuscular level [32,42]. This is probably due to suboptimal electroporation conditions caused by the use of an *in ovo*, rather than *in vivo*, electroporator.

The dosage selection for systemic administration was based on the disease pathogenesis and the mode of action of our LNA/2′*O*Me chimeras. For RNA-degrading gapmer ASOs against *Dmpk* mRNA, dosages as low as 25 mg/kg/week have been reported [37]. Given that a single gapmer ASO molecule can target and degrade many mRNA molecules, lower drug amounts would be required to achieve an effect. By contrast, a steric-blocking ASO will remain bound to a single target site, thus increasing the number of ASO molecules needed to elicit an effect. The situation is further amplified in the case of DM1, where dozens of steric-blocking ASO molecules would be required to inhibit MBNL1 sequestration to a level that restores alternative splicing regulation. To our knowledge, the highest reported dosage of a naked, steric-blocking ASO delivered systemically was 200 mg/kg/week, to induce *dystrophin* (*Dmd*) exon 23 skipping in the mdx mouse model of Duchenne muscular dystrophy (DMD) [43]. We therefore decided to proceed with a dosage regimen of 200 mg/kg per injection, administered subcutaneously two times a week for 4 weeks.

Despite high accumulation levels in skeletal muscle tissues, comparable with those reported in Goyenvalle *et al.* for tricyclo-DNA oligomer against *Dmd*, our chimeric

FIG. 5. **(A, B)** Tissue weights and plasma biochemistry analyses in WT, HSA^{LR} control, and ASO-treated HSA^{LR} mice ($n = 3$ per group). Plasma levels of CPK, AST, ALT, BUN, and creatinine in HSA^{LR} mice were measured 2 days after treatment with saline only or 200 mg/kg of the indicated ASO, twice a week for 4 weeks. Values are expressed as the mean ± S.E.M. **(C)** Histopathological assessment of liver and kidney tissues from HSA^{LR} mice treated with 200 mg/kg of the indicated ASO, biweekly for 4 weeks. Representative sections stained with hematoxylin and eosin. **(iii)** *White arrowheads* indicate mild multifocal necrosis in proximal convoluted tubules in a mouse treated with LNAc/2′*O*Me14. **(v)** Randomly distributed, mild hepatocellular necrosis and focal periportal lymphocytic infiltration (*yellow arrowhead*) in a mouse treated with LNAc/2′*O*Me18h. **(vi)** Mild centrilobular necrosis (*white arrowheads*) in the liver tissue of an LNAc/2′*O*Me14-treated mouse. ALT, alanine aminotransferase; AST, aspartate aminotransferase; BUN, blood urea nitrogen; CPK, creatine phosphokinase; WT, wild type. Color images are available online.

A

	Treatment group		
	Saline	LNAc/2´OMe18h	LNAc/2´OMe14
Body weight (g)			
Beginning	23.33 ± 1.333	24.67 ± 0.333	22.33 ± 0.333
Endpoint	24.33 ± 1.453	27.00 ± 0.577	25.00 ± 0.000
Tissue weights (g)			
Liver	1.19 ± 0.085	1.41 ± 0.083	1.51 ± 0.009
Kidney	0.15 ± 0.004	0.17 ± 0.003	0.17 ± 0.000
Spleen	0.09 ± 0.009	0.12 ± 0.010	0.11 ± 0.005

B

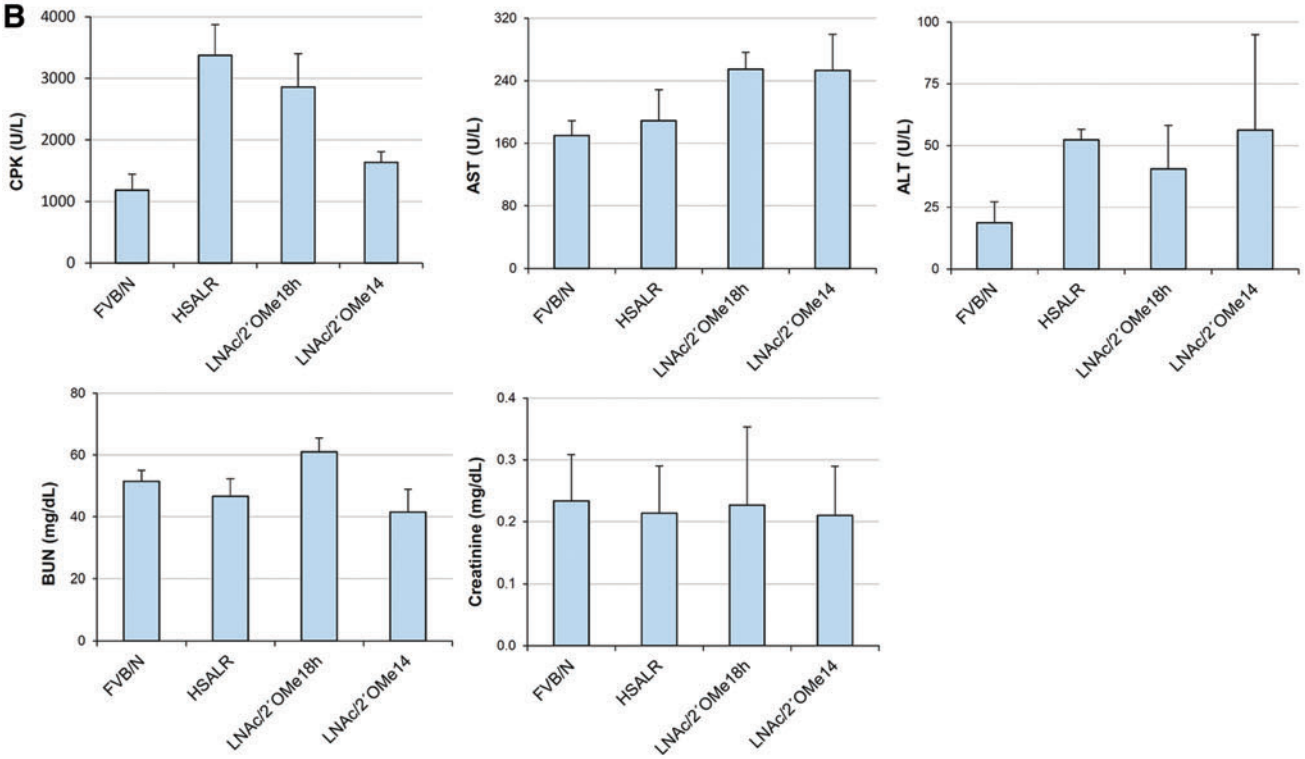

C

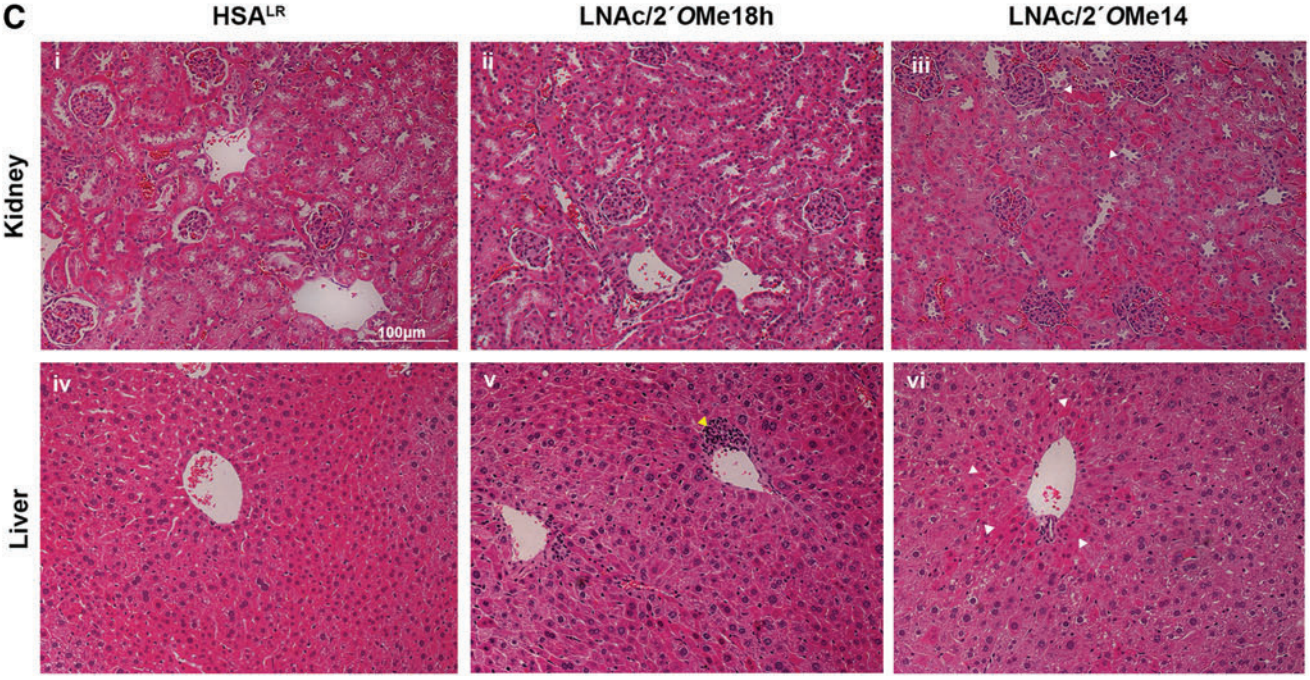

LNA/2′*O*Me ASOs were unable to reduce the number of CUG^{exp}-Mbnl1 foci and reverse *Serca1* exon 22 missplicing in skeletal muscle tissues. Before this study, Leger *et al.* were the only group to demonstrate complete reversal of misregulated *Serca1* alternative splicing after systemic administration of a peptide-linked, steric-blocking morpholino ASO in HSA^{LR} mice [39]. Importantly, when administered naked, the ASO failed to show any improvement in *Serca1* missplicing in all tested skeletal muscles. These results imply that in the absence of a tissue-targeting conjugate, ASO uptake is not sufficient to enable intracellular efficacy.

The covalent attachment of cationic cell-penetrating peptides (CPPs) to charge-neutral steric-blocking ASOs—for example, morpholino—has shown to considerably enhance ASO uptake and activity in DM1 and DMD mouse models [39,44,45]. However, this is very much restricted to charge-neutral chemistries, as conjugation of cationic CPPs to anionic PS-modified ASOs would lead to electrostatic interactions, causing self-aggregation and disrupted binding to the target region. Consequently, in an attempt to increase ASO delivery and *Dmpk* mRNA degradation in DM1 muscle tissues, Ionis Pharmaceuticals and collaborators proceeded with the introduction of a lipid-based motif (5′-*N*-Palmitoylhexylamino) to the 5′ end of their PS-modified gapmer [46]. Conjugation of a hydrophobic cell-penetrating ligand to our chimeric LNA/2′*O*Me ASOs could therefore enhance uptake in skeletal muscle tissues to a level that elicits a corrective effect. However, it is still questionable whether this approach would be more effective than a ligand-conjugated RNA-degrading ASO.

A critical step in the success of oligonucleotide therapies is the implementation of early screening strategies to address potential toxicologic effects. The mechanisms by which ASOs can cause cellular toxicity can be classified in two categories: (1) hybridization-dependent toxicity caused by ASO binding to a partially complementary, off-target sequence and (2) hybridization-independent toxicity, which includes dose-related hyperaccumulation, and immunostimulatory and aptameric binding effects [47]. All types of toxicities are highly dependent on the sequence and the modification pattern of the individual ASO. Despite the high-dosage regimen used, corresponding to a cumulative dose of 3.2 g/kg, our 18mer and 14mer LNA/2′*O*Me ASOs showed minimal hepatotoxicity based on minor histological lesions and slightly elevated AST levels. Previous studies of LNA-modified gapmer ASOs have shown significantly elevated levels of hepatic transaminases (ALT/AST), profound histological lesions, and, in some cases, early morbidity, at cumulative doses of 100 mg/kg (ie, a more than 30-fold lower dose than the one administered in our study) [33–35]. Considering the different modification pattern and mode of action of LNA/DNA gapmer ASOs versus LNA/2′*O*Me chimeras, a direct toxicologic comparison would not be justified. Nevertheless, we can safely argue that hyperaccumulation of steric-blocking chimeric LNA/2′*O*Me ASOs does not appear to cause any profound hybridization-independent toxicity in liver and kidney tissues.

To conclude, our study demonstrates that direct inhibition of Mbnl1 sequestration by systemic delivery of chimeric LNA/2′*O*Me ASOs is an ineffective approach for DM1 therapy. Nevertheless, the data obtained open prospects for the application of LNA/2′*O*Me chimeras as steric-blocking agents for the treatment of other diseases. The combinatory introduction of LNA and 2′*O*Me chemistries to a fully modified PS backbone did not cause profound histological toxicity and resulted in relatively high levels of ASO accumulation in skeletal muscles, diaphragm, and heart tissue. Therefore, in the concept of a much simpler pathogenic model that requires inhibition of a single target site per RNA molecule, chimeric LNA/2′*O*Me ASOs could prove to be highly beneficial and safe.

Acknowledgments

The authors thank Professor Charles A. Thornton for providing us with the HSA^{LR} mouse model. Special thanks go to Mrs. Revecca Papacharalambous for the tissue embedding and Ms. Chrystalla Kamma for the sectioning and H&E staining.

Author Disclosure Statement

No competing financial interests exist.

Funding Information

This work was supported by grants to L.A.P. and N.P.M. from the A.G. Leventis Foundation and AFM, respectively.

Supplementary Material

Supplementary Table S1

References

1. Udd B and R Krahe. (2012). The myotonic dystrophies: molecular, clinical, and therapeutic challenges. Lancet Neurol 11:891–905.
2. Meola G and R Cardani. (2015). Myotonic dystrophies: an update on clinical aspects, genetic, pathology, and molecular pathomechanisms. Biochim Biophys Acta 1852:594–606.
3. Mahadevan M, C Tsilfidis, L Sabourin, G Shutler, C Amemiya, G Jansen, C Neville, M Narang, J Barceló, *et al.* (1992). Myotonic dystrophy mutation: an unstable CTG repeat in the 3′ untranslated region of the gene. Science 255:1253–1255.
4. Pettersson OJ, L Aagaard, TG Jensen and CK Damgaard. (2015). Molecular mechanisms in DM1—a focus on foci. Nucleic Acids Res 43:2433–2441.
5. Charlet BN, RS Savkur, G Singh, AV Philips, EA Grice and TA Cooper. (2002). Loss of the muscle-specific chloride channel in type 1 myotonic dystrophy due to misregulated alternative splicing. Mol Cell 10:45–53.
6. Ho TH, BN Charlet, MG Poulos, G Singh, MS Swanson and TA Cooper. (2004). Muscleblind proteins regulate alternative splicing. EMBO J 23:3103–3112.
7. Kino Y, C Washizu, M Kurosawa, Y Oma, N Hattori, S Ishiura, and N Nukina. (2015). Nuclear localization of MBNL1: splicing-mediated autoregulation and repression of repeat-derived aberrant proteins. Hum Mol Genet 24: 740–756.
8. Philips AV, LT Timchenko and TA Cooper. (1998). Disruption of splicing regulated by a CUG-binding protein in myotonic dystrophy. Science 280:737–741.
9. Savkur RS, AV Philips and TA Cooper. (2001). Aberrant regulation of insulin receptor alternative splicing is

associated with insulin resistance in myotonic dystrophy. Nat Genet 29:40–47.
10. Freyermuth F, F Rau, Y Kokunai, T Linke, C Sellier, M Nakamori, Y Kino, L Arandel, A Jollet, *et al.* (2016). Splicing misregulation of SCN5A contributes to cardiac-conduction delay and heart arrhythmia in myotonic dystrophy. Nat Commun 7:11067.
11. Stein CA, C Subasinghe, K Shinozuka and JS Cohen. (1988). Physicochemical properties of phosphorothioate oligodeoxynucleotides. Nucleic Acids Res 16:3209–3221.
12. Beltinger C, HU Saragovi, RM Smith, L LeSauteur, N Shah, L DeDionisio, L Christensen, A Raible, L Jarett and AM Gewirtz. (1995). Binding, uptake, and intracellular trafficking of phosphorothioate-modified oligodeoxynucleotides. J Clin Invest 95:1814–1823.
13. Geary RS, RZ Yu and AA Levin. (2001). Pharmacokinetics of phosphorothioate antisense oligodeoxynucleotides. Curr Opin Investig Drugs 2:562–573.
14. Cazenave C, CA Stein, N Loreau, NT Thuong, LM Neckers, C Subasinghe, C Hélène, JS Cohen and JJ Toulmé. (1989). Comparative inhibition of rabbit globin mRNA translation by modified antisense oligodeoxynucleotides. Nucleic Acids Res 17:4255–4273.
15. Brown DA, SH Kang, SM Gryaznov, L DeDionisio, O Heidenreich, S Sullivan, X Xu and MI Nerenberg. (1994). Effect of phosphorothioate modification of oligodeoxynucleotides on specific protein binding. J Biol Chem 269: 26801–26805.
16. Weidner DA, BC Valdez, D Henning, S Greenberg and H Busch. (1995). Phosphorothioate oligonucleotides bind in a non sequence-specific manner to the nucleolar protein C23/nucleolin. FEBS Lett 366:146–150.
17. Shen W, XH Liang and ST Crooke. (2014). Phosphorothioate oligonucleotides can displace NEAT1 RNA and form nuclear paraspeckle-like structures. Nucleic Acids Res 42:8648–8662.
18. Liang XH, H Sun, W Shen and ST Crooke. (2015). Identification and characterization of intracellular proteins that bind oligonucleotides with phosphorothioate linkages. Nucleic Acids Res 43:2927–2945.
19. Liang XH, W Shen, H Sun, GA Kinberger, TP Prakash, JG Nichols and ST Crooke. (2016). Hsp90 protein interacts with phosphorothioate oligonucleotides containing hydrophobic 2′-modifications and enhances antisense activity. Nucleic Acids Res 44:3892–3907.
20. Gao WY, FS Han, C Storm, W Egan and YC Cheng. (1992). Phosphorothioate oligonucleotides are inhibitors of human DNA polymerases and RNase H: implications for antisense technology. Mol Pharmacol 41:223–229.
21. Yaswen P, MR Stampfer, K Ghosh and JS Cohen. (1993). Effects of sequence of thioated oligonucleotides on cultured human mammary epithelial cells. Antisense Res Dev 3:67–77.
22. Sarmiento UM, JR Perez, JM Becker and R Narayanan. (1994). In vivo toxicological effects of rel A antisense phosphorothioates in CD-1 mice. Antisense Res Dev 4:99–107.
23. Galbraith WM, WC Hobson, PC Giclas, PJ Schechter and S Agrawal. (1994). Complement activation and hemodynamic changes following intravenous administration of phosphorothioate oligonucleotides in the monkey. Antisense Res Dev 4:201–206.
24. Agrawal S, PK Rustagi and DR Shaw. (1995). Novel enzymatic and immunological responses to oligonucleotides. Toxicol Lett 82–83:431–434.
25. Shen W, De CL Hoyos, MT Migawa, TA Vickers, H Sun, A Low, TA Bell 3rd, M Rahdar, S Mukhopadhyay, *et al.* (2019). Chemical modification of PS-ASO therapeutics reduces cellular protein-binding and improves the therapeutic index. Nat Biotechnol 37:640–650.
26. Monia BP, EA Lesnik, C Gonzalez, WF Lima, D McGee, CJ Guinosso, AM Kawasaki, PD Cook, SM Freier, *et al.* (1993). Evaluation of 2′-modified oligonucleotides containing 2′-deoxy gaps as antisense inhibitors of gene expression. J Biol Chem 268:14514–14522.
27. Mulders SA, WJ van den Broek, TM Wheeler, HJ Croes, P van Kuik-Romeijn, SJ de Kimpe, D Furling, GJ Platenburg, G Gourdon, *et al.* (2009). Triplet-repeat oligonucleotide-mediated reversal of RNA toxicity in myotonic dystrophy. Proc Natl Acad Sci U S A 106:13915–13920.
28. Kauppinen S, B Vester and J Wengel. (2005). Locked nucleic acid (LNA): high affinity targeting of RNA for diagnostics and therapeutics. Drug Discov Today Technol 2: 287–290.
29. Kumar R, SK Singh, AA Koshkin, VK Rajwanshi, M Meldgaard and J Wengel. (1998). The first analogues of LNA (locked nucleic acids): phosphorothioate-LNA and 2′-thio-LNA. Bioorg Med Chem Lett 8:2219–2222.
30. Kamola PJ, JD Kitson, G Turner, K Maratou, S Eriksson, A Panjwani, LC Warnock, GA Douillard Guilloux, K Moores, *et al.* (2015). In silico and in vitro evaluation of exonic and intronic off-target effects form a critical element of therapeutic ASO gapmer optimization. Nucleic Acids Res 43:8638–8650.
31. Kurreck J, E Wyszko, C Gillen and VA Erdmann. (2002). Design of antisense oligonucleotides stabilized by locked nucleic acids. Nucleic Acids Res 30:1911–1918.
32. Wojtkowiak-Szlachcic A, K Taylor, E Stepniak-Konieczna, LJ Sznajder, A Mykowska, J Sroka, CA Thornton and K Sobczak. (2015). Short antisense-locked nucleic acids (all-LNAs) correct alternative splicing abnormalities in myotonic dystrophy. Nucleic Acids Res 43:3318–3331.
33. Swayze EE, AM Siwkowski, EV Wancewicz, MT Migawa, TK Wyrzykiewicz, G Hung, BP Monia and CF Bennett. (2007). Antisense oligonucleotides containing locked nucleic acid improve potency but cause significant hepatotoxicity in animals. Nucleic Acids Res 35:687–700.
34. Stanton R, S Sciabola, C Salatto, Y Weng, D Moshinsky, J Little, E Walters, J Kreeger, D DiMattia, *et al.* (2012). Chemical modification study of antisense gapmers. Nucleic Acid Ther 22:344–359.
35. Burdick AD, S Sciabola, SR Mantena, BD Hollingshead, R Stanton, JA Warneke, M Zeng, E Martsen, A Medvedev, *et al.* (2014). Sequence motifs associated with hepatotoxicity of locked nucleic acid—modified antisense oligonucleotides. Nucleic Acids Res 42:4882–4891.
36. Wheeler TM, AJ Leger, SK Pandey, AR MacLeod, M Nakamori, SH Cheng, BM Wentworth, CF Bennett and CA Thornton. (2012). Targeting nuclear RNA for in vivo correction of myotonic dystrophy. Nature 488:111–115.
37. Pandey SK, TM Wheeler, SL Justice, A Kim, HS Younis, D Gattis, D Jauvin, J Puymirat, EE Swayze, *et al.* (2015). Identification and characterization of modified antisense oligonucleotides targeting DMPK in mice and nonhuman primates for the treatment of myotonic dystrophy type 1. J Pharmacol Exp Ther 355:329–340.

38. Madsen A. (2017). Ionis Reports Setback on DMPKRx Program for Myotonic Dystrophy. https://strongly.mda.org/
39. Leger AJ, LM Mosquea, NP Clayton, IH Wu, T Weeden, CA Nelson, L Phillips, E Roberts, PA Piepenhagen, SH Cheng and BM Wentworth. (2013). Systemic delivery of a Peptide-linked morpholino oligonucleotide neutralizes mutant RNA toxicity in a mouse model of myotonic dystrophy. Nucleic Acid Ther 23:109–117.
40. Rosenblatt JD, AI Lunt, DJ Parry and TA Partridge. (1995). Culturing satellite cells from living single muscle fiber explants. In Vitro Cell Dev Biol Anim 31:773–779.
41. Le BT, AM Adams, S Fletcher, SD Wilton and RN Veedu. (2017). Rational design of short locked nucleic acid-modified 2′-O-methyl antisense oligonucleotides for efficient exon-skipping in vitro. Mol Ther Nucleic Acids 9: 155–161.
42. Wheeler TM, K Sobczak, JD Lueck, RJ Osborne, X Lin, RT Dirksen and CA Thornton. (2009). Reversal of RNA dominance by displacement of protein sequestered on triplet repeat RNA. Science 325:336–339.
43. Goyenvalle A, G Griffith, A Babbs, S El Andaloussi, K Ezzat, A Avril, B Dugovic, R Chaussenot, A Ferry, *et al.* (2015). Functional correction in mouse models of muscular dystrophy using exon-skipping tricyclo-DNA oligomers. Nat Med 21:270–275.
44. Betts C, AF Saleh, AA Arzumanov, SM Hammond, C Godfrey, T Coursindel, MJ Gait and MJA Wood. (2012). Pip6-PMO, a new generation of peptide-oligonucleotide conjugates with improved cardiac exon skipping activity for DMD treatment. Mol Ther Nucleic Acids 1:e38.
45. Klein AF, MA Varela, L Arandel, A Holland, N Naouar, A Arzumanov, D Seoane, L Revillod, G Bassez, *et al.* (2019). Peptide-conjugated oligonucleotides evoke long-lasting myotonic dystrophy correction in patient-derived cells and mice. J Clin Invest 129:4739–4744.
46. Mignon L. (2017). IONIS-DMPKRx Clinical Program in Myotonic Dystrophy. https://www.myotonic.org/sites/default/files/MDF_Mignon_09Sep2017.pdf
47. Frazier KS. (2015). Antisense oligonucleotide therapies: the promise and the challenges from a toxicologic pathologist's perspective. Toxicol Pathol 43:78–89.

Address correspondence to:
Leonidas A. Phylactou, PhD
The Cyprus School of Molecular Medicine
The Cyprus Institute of Neurology and Genetics
P.O. Box 23462
Nicosia 1683
Cyprus

E-mail: laphylac@cing.ac.cy

Received for publication July 4, 2019; accepted after revision November 13, 2019.